Dr. Renée Heilbronner

Handling Topical Editor, Solid Earth

Dear Renée Heilbronner,

We are pleased to submit a revised version of this manuscript, entitled 'Structural Disorder of Graphite and Implications for Graphite Thermometry' to you, for consideration for publication in Solid Earth.

Herein, we investigated the possibility of mechanical modifications of graphite structure in laboratory deformation experiments. We document systematic decrease in graphite crystallinity as a function of increasing shear strain during shear experiments with aseismic sliding velocities. Our results contradict the paradigm that the degree of graphite crystallinity is determined by irreversible maturation of carbonaceous material. This finding has implications for the calibrated graphite 'thermometer' as mechanically induced disorder of the graphite structure may lead to temperature calculations that significantly underestimate the peak metamorphic temperatures in deformed rocks. Therefore, we suggest that the current graphite 'thermometer' should be re-evaluated.

We have substantially revised the manuscript taking into account reviewer`s suggestions, as well as some ideas that have been discussed among co-authors in the months since first submission. In particular, we further examined the nature of the processes that operated during shearing and resulted in the documented structural disorder of graphite by implementing transmission electron microscopy. Also, we have added Toru Takeshita as a co-author because of his valuable contribution to the current manuscript.

We have copied the reviews below and addressed each comment in turn. Our responses are indicated in green text. We have also used track changes to document revisions to the manuscript and are resubmitting both a track changes, and changes accepted versions. We refer to revisions in the manuscript by line numbers – these are correct with respect to the revised version with changes accepted.

Thank you for your consideration of this manuscript.

Regards,

Martina Kirilova
Corresponding Author
martina.a.kirilova@gmail.com

On behalf of the authors: Virginia Toy, Jeremy S. Rooney, Carolina Giorgetti, Keith C. Gordon, Cristiano Collettini and Toru Takeshita.

Interactive comment on "Structural Disorder of Graphite and Implications for Graphite Thermometry" by Martina Kirilova et al.

Dr. Kilian (Referee)

ruediger.kilian@unibas.ch

Received and published: 24 July 2017

In the manuscript "Structural Disorder of Graphite and Implications for Graphite Thermometry" s2-2017-74, Kirilova et al. report the results of Raman spectroscopy on an experimentally sheared, synthetic graphite gouge. Raman spectroscopy on carbonaceous material (RSCM) has become a frequently used geothermometer assuming that the crystallinity of graphite represents peak metamorphic conditions. In contrast to geothermometers based on mineral compositions where a retrograde overprint can often be easily recognized, preservation of peak metamorphic conditions under deformation might not be easily recognised in graphite where no compositon changes are to be expected. Accordingly, this contribution is of special interest to researchers, either using RSCM or having to evaluate RSCM derived data. Testing the RSCM thermometer against experimentally deformed graphite gouge is novel and the results of the presented study are very interesting and strongly suggest that the applicability RSCM thermometry to deformed rocks - and accordingly to almost all metamorphic rocks - needs a careful evaluation. This ms highlights that not all parameters to unequivocally interpret RSCM are sufficiently understood. The authors of the ms suggest a correction of the RSCM thermometer based on shear strain, related to their observations in the synthetic graphite gouge.

The manuscript is concise, easy to read and provides a valuable insight into a neglected problem of RSCM. However, there are points that are either not entirely consistent, that need further clarification or corrections, especially in the obtained relation to sample strain and the determination of crystallinity and those should be addressed (listed below). Overall I recommend that the manuscript is suitable for publication after moderate revisions.

Following comments should be addressed.

1) Relation to strain/stress
a) A "shear strain" is calculated by summing up the ratios of displacement increments and thickness. As it appears the samples are thinning with increasing displacement, this "shear strain" is neglecting the thinning component, the derived "shear strain" cannot be used to calculate a strain ellipse (no functional relation) and overestimates strain in the sample. A more correct procedure would be one where progressive simple and pure shear are treated to occur concurrently, and reporting a unique measure of strain.

Response:
By "measured layer thickness" we mean the layer thickness measured at the same record number at which the shear displacement increments were measured, i.e. it is the instantaneous layer thickness. Consequently, we take into account the sample thinning with increasing displacement. Perhaps we need to better explain this in the manuscript.

However, we recognize that you have recently recalculated strains in simple shear experiments that take the layer thinning into account (Kilian, R., & Heilbronner, R. 2017, April. Texture transition in experimentally deformed quartzite. In EGU General Assembly Conference

Abstracts, Vol. 19, p. 6966). We hope you can advise us in more detail how we could most appropriately make use of such calculations in our current study.

Reply to Response:

Summing up individual steps (delta displacement/current thickness) does not produce a shear strain which accounts for the deformation imposed on the sample. This measure could be termed "apparent shear strain" but it overestimates the true (shear) strain. This apparent shear strain cannot be used to derive a strain ellipse (and accordingly strain related measures i.e. LINFS, ISA, ... any measure of strain). Any correlations of e.g. microstructural features or any other supposedly strain dependent material property should greatly benefit from a correct measure of strain. For a simple procedure to derive bulk strain under the assumption of simultaneous thinning and shearing see e.g. Fossen&Tikoff (1993).

Response 2: Thank you for the additional explanation and the reference provided. In support to our shear strain estimates we have also calculated total frictional work as suggested by Reviewer 2 to avoid this issue.

b) The authors report (and obtain their measurements) from the shiny surface where they assume along which most of the displacement is realised. Assuming that this surface is actually a thin layer, the strain within that layer must always be larger than the strain derived from the entire sample. Hence one might speculate that a functional relation between the determined "shear strain" and R2 is at best a rough approximation. In case, as indicated by some of the comments on the microstructure, the compaction (sample thinning?) is localised as well and not homogeneous, a bulk sample, "strain estimate" is even more likely to be unrelated to the state of deformation in the analysed layer.

Response:

We agree with your statement that the measured bulk shear strain is most probably significantly lower than the shear strain accumulated only within the thin shear surfaces. However, we expect the shear strain variations within these surfaces to be linearly correlated with the measured bulk shear strain within a sample. Thus, we believe that a correlation between shear strain and R2 is in fact possible. Nevertheless, we will relate to this relationship as a ‘rough approximation’.

Additionally, brittle deformation in most fault gouges is observed to occur in a localized way, with displacement focused on a series of through-going and anastomosing shear surfaces (Craw and Upton, 2014). In polyphase gouges, graphite is quite commonly focused into these anastomosing shear surfaces (e.g. Nakamura et al., 2015; Kirilova et al., in press). So, in any natural fault that may have experienced a shear strain that we measure from its total displacement and the thickness of the deforming zone, it is also likely that individual graphite-bearing layers actually accommodated much higher shear strains, probably similar to the ones

in our experiments. Therefore, correlation between bulk shear strain and R2 may actually be quite a good approximation because it is applicable to complex natural systems.

Reply to Response:

(a) It is unclear to me, on what base the relationship between bulk (sample) strain and strain within the thin, deforming layer(s) should be linear over the range of all experiments. Is the number and the thickness of these layers known and if so, are they always constant? Otherwise, to my opinion a linear relation appears to be speculative.

(b) The complexity of a naturally deformed, polymineralic rock where graphite may form layers (which may tend to localize strain, which may be arranged in an anastomosing network and which may differ in thickness and hence experience a large variation in strain) is not necessarily identical to the situation in the experiments. Simply because an experiment is a complex, it's complexity may not automatically balance the complexities found in nature. Certainly, there's a good chance that deformation localizes into graphite layers in nature, but it remains unclear to me why this should occur at the same (linear? as proposed above) ratio with respect to bulk strain as in the pure graphite experiments. It remains unclear to me why it should be likely that in a polymineralic rock, strain partition would between graphite and e.g. quartz in a similar way as in a pure graphite system.

Response 2: In our experimental samples these layers tend to form at systematic spacing controlled by the spacing of teeth on the forcing blocks. However, we acknowledge that the strain accommodated within each shiny surface will be much higher than the bulk strain accommodated by the gouge layer. This is now acknowledged in lines 214-216. Furthermore, polyphase natural gouges that comprise anastomosing networks of localised shear zones between more rigid clasts will also contain graphite layers that accommodate greater strains individually than the bulk strain within the layer. However, we recommend that the relationship we have determined can only be directly applied to natural cases if the spacing and thickness of localised layers compared to total layer thickness is similar to that of our experiments.

c) The authors use a mixture of surface related measures (friction coefficients, normal stress, slip rate) and volume measures (strain) which might be confusing in places, e.g. it might not be directly evident that the experiments with the 25 MPa normal stress should actually be stronger that the 5 MPa experiments.

Response:
With our mechanical data, presented in Figure 1, we are using standard measurements, i.e. double direct shear experiments on powdered material, to test the frictional properties of graphite. The vast literature (Brace & Byerlee, 1966; Byerlee 1978; Blampied et al., 1995; Marone, 1998; etc.) that put the base for fault strength is based on experiments similar to those

presented in our work. Our experiments are performed at different values of normal stress (5 and 25 MPa) and at different sliding velocities (1-10-100 microns/s), and represent the deformation of a shear zone that has an initial thickness of 3 mm. In all the experiments with increasing displacement, i.e. with increasing strain, we observe an initial phase of strengthening until a peak stress is reached, then we observe strain weakening until a steady state friction is achieved. Mechanical data clearly show that: 1) Friction coefficient is lower at high normal stress and this means that the experimental fault at 25 MPa is weaker than the one at 5 MPa; 2) The sliding velocity does not influence too much the frictional properties of the experimental fault. During deformation, a typical fabric develops within the entire shear zone (e.g. Marone, 1998, fig 11) and the fault strength is strongly related to fabric evolution. In other words, frictional strength, fabric and strain are strongly connected.

Reply to Response:

The answer of the authors reflects that a mixture of surface properties and strain is indeed confusing. Frition coefficients give a ratio of shear to normal stress but are not a measure of the actual strength of a volume of rock. Expressing sample "strength" in terms of friction coefficient may be more appropriate if it is assumed that the sample is actually deforming only along a surface, however in that case the concept of strain is not existent.

Besides all, for the main and important part of the manuscript, I think the mechanical data (displacement-friction coefficient or strain-shear stress) are only relevant to make any point that the samples are deforming by a brittle, semi-brittle or ductile mechanism. The measures of strain (and in this case, estimates of strain inside the deforming layers of the sample) are those relevant to the points addressed in (2), the relation between Raman spectra and strain.

Response 2: We agree with your comment.

2) R2 correlation with shear strain
a) Following the number in formula 1 and as shown in Figure 3., shear shear is evaluated as a function of R2, the inverse would be logical and a fit is numerically not equivalent. Additionally, formula 1 is wrong.

Response:
We plotted R2 as a function of shear strain and fitted the curve one more time. On Figure 3_version 2 (attached) you can see the resulting figure together with the new formula, which was automatically calculated by Excel. Could you please advise us if the revised version of the figure is correct?

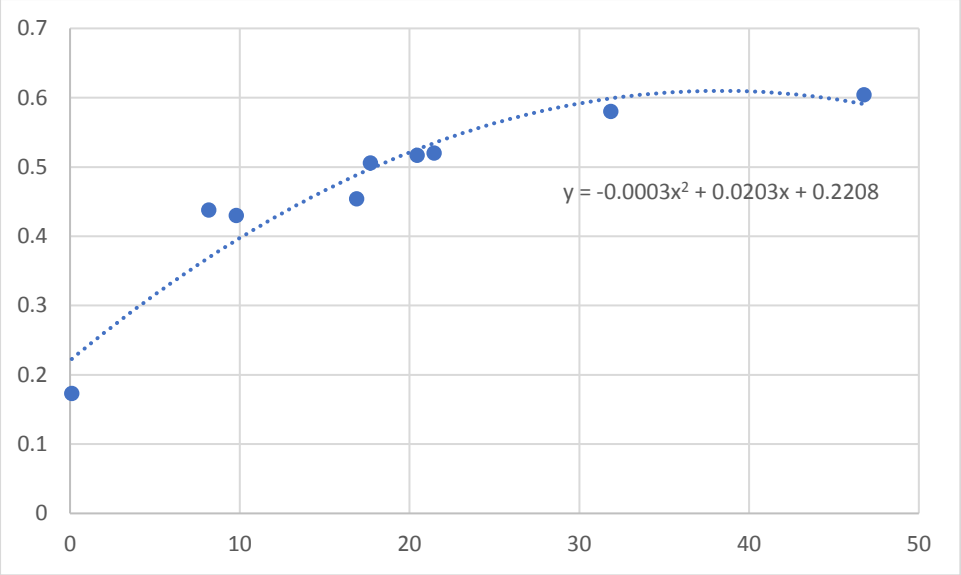

b) What is the physical basis that R2 and strain should have a power law relationship?

Response:

If we take the R2 value associated with fitting of a curve in Excel as a measure, then a power law function provides the best fit to the relationship between shear strain and R2. It may be possible to fit the curve using other types of equations, and we are open to your suggestions on what other functions we should try.

Reply to Response:

The way data is evaluated (R2 as a function of "strain" and not the other way around) is now correct. However, why should it have now a quadratic relationship. At high shear strain, R2 will decrease again (also visible in your new plot)! So the way to evaluate the data (R2=f(strain)) is correct, a quadratic fit however does not really make sense to me.

Response 2: Thank you for this comment. We plotted the figure by using Matlab instead of Excel, and we achieved much better results. This relationship is now described by a power function.

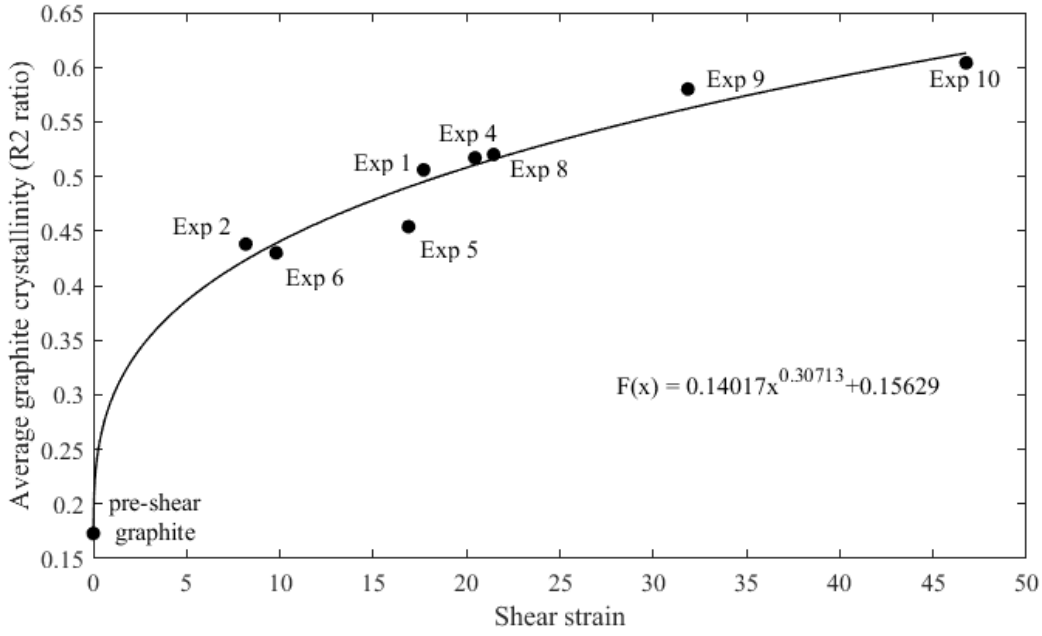

3) Origin of D1,2 bands Obtaining Raman spectra at surface ledges on (001) or generally grain boundary regions, the appearance of the D bands has been observed (e.g.Tuinstra & Koenig, 1970; Pimenta et al. 2007). For small grain sizes, the ratio of G and D bands is actually used to establish a grain size determination. The authors mention that the increasing area of D1, D2 peaks is related to a decreasing crystallinity of graphite, is it possible that the crystallinity does not change but rather with a smaller grain size more grain boundary area with a disturbed lattice is measured? The authors estimate the minimum resolution of their optical system at 0.4 _m, however, from the text it becomes not clear whether this relates to the analysed point and/or if the analysed point could actually be identified and if so, whether measurements with a large R2 come from areas with a smaller grain size? If crystallinity is defined in relation to intragranular defect density/lattice perfection, it should be verified that only intragranular measurements are evaluated. If the grainsize is so small that most likely grain aggregates are measured, maybe the grain size effect could be corrected. The authors mention that they actually examine the structural disordering of graphite, so depending how this is defined, it needs to be considered separately to grain boundary effects.

Response:

We acknowledge that the measured increase in D bands can result both from (1) decrease in crystallinity and (2) spectra obtained on grain boundaries. Furthermore, more surfaces are likely to be created as a result of brittle deformation. In addition, in natural fault zones graphite commonly appears with significantly smaller grain size (e.g. <1 micron in the Alpine Fault cataclasites; Kirilova et al, in press) than in our experimental samples. Thus, the calibrated Raman thermometer could yield temperatures that significantly underestimate the peak metamorphic temperatures experienced by the host rocks. Nevertheless, our experimental study proves that the calibrated Raman thermometers are unreliable in active tectonic settings.

However, in our study: (1) We attempted to avoid grain boundaries as much as possible, and thus most (if not all) of our measurements were obtained from intragranular areas; (2) our SEM data (fig. 4b) shows that the accumulated shear surfaces are compiled of grains > 10 microns in size, which is significantly larger than the laser spot size (approximately 412 nm). Therefore,

we believe that the detected increase of D bands in our experimental data in fact reflects disorder of the internal structure of graphite rather than grain size reduction.

Reply to Response:

Both, a strongly reduced grain size as well as a reduced crystallinity will certainly lead to increased D bands and an underestimation of a RSCM temperature; this is the important message in the manuscript. However, based on the presented data, I do not clearly see how the two possible effects could be separated. It was mentioned in the manuscript that the intent was to avoid grain boundaries, however, to me it is not clear how this was done. Inspecting e.g. Figures 4a, a BSE image, I find it difficult to detect grains or grain boundaries. Are grain boundaries so much more obvious is the LM images of the Raman system? Is the assumed grain size of 10-50 µm really present in the thin deforming layers which were actually measured. A nice micrograph showing these features would be quite helpful.

Response 2: We show the size of grains comprising the shiny surface clearly in Figure 4b. Furthermore, the overall crystallinity of a sample will naturally reduce with grain size reduction since that increases the grain surface (volume ratio and grain surfaces are much less crystalline than their interiors).

4) Applicability of a strain corrected RSCM thermometer
a) in real rocks, it might be difficult to estimate strain and it might not be clear in which way deformation partitions between graphite and other minerals and so I'd encourage the authors to share some thoughts on how a strain correction should be applicable in a real-rock situation.

Response:

We agree that estimating shear strain in real rocks could be a challenging task. Therefore, the suggested calibration could be used only in the case when shear strain can be undoubtedly identified. Furthermore, in the initial version of the manuscript we acknowledge the importance of sliding velocities, and thus suggest that shear strain calibration may not be sufficient for reliable temperature estimates in active tectonic settings (lines 304-308).

Reply to Response:

a) It is often challenging to derive a reliable strain measure from a natural rock (even when neglecting e.g. a complex deformation-uplift history). Following the earlier arguments, I think it is even more challenging to estimate the strain that an individual graphite seam inside such a rock may have experienced. Assuming that the authors would establish their "strain-R2"-relation based on an estimate of the strain in the thin deforming layer, it would still be very

difficult in natural cases to "undoubtedly identify" strain accumulated in the graphite seams. I think this is a sufficiently complex problem without actually having to start thinking about any effect of deformation rates (not sliding rates) or other parameters.

Response 2: We are glad you agree.

b) A correction for the thermometer might depend on the relation of temperature and strain: e.g. during exhumation of a rock deformation takes place at increasingly lower temperature. Using a simple "strain" correction, would imply that the deformation temperatures during exhumation would not have to be considered. Given that most minerals show different deformation mechanisms at different temperatures, it might be reasonable to assume that this is the case as well for graphite. So strictly speaking, a correction should only consider lattice defects introduced by the identical process which is occurring in the calibration experiments. I'd encourage the authors to comment on this complication of such an effort.

Response: As you have mentioned during exhumation of a rock, deformation takes place at increasingly lower temperature. However, graphite structure is sensitive only to increase in temperature i.e. graphite crystallinity increases with increasing temperature. Retrograde metamorphism is known not to affect the degree of graphite crystallinity that has been previously achieved. Thus, in the suggested scenario the accumulated shear strain will be the main parameter affecting graphite structural order. On the contrary, we expect that shear strain in high temperature conditions would yield significantly different results than the ones presented in our study.

Reply to Response:

b) This comment was not about the effect of retrograde metamorphism but rather on the effect of exhumation at increasingly lower temperatures, where it is not well known when brittle behaviour of graphite starts to dominant. The presented experiments nicely demonstrate that graphite deformed at room temperature shows a reduced RSCM temperature. Despite graphite deformation at higher temperature might indeed be a different story, it is primarily very challenging to identify the part of deformation accumulated in a graphite layer which was established under brittle conditions in order to apply the "strain-correction" derived by the presented, supposedly brittle experiments. I can perfectly imagine that higher temperature deformation does a similar RSCM temperature resetting to graphite, but there might be a different functional relation compared to the one which is intended in the present study.

Response 2: True. We did already acknowledge that ductile as well as brittle mechanisms may impact the thermometric calibration, but we don't have data to address that in the current study (lines 275-279).

c) Using any thermometer to determine peak temperatures, often the measurements yielding the highest results are considered as representing peak conditions to overcome the problem of a partial lower temperature overprint. Given that some measurements in deformed samples still yield a low R2, it would be helpful to see where those measurements are actually determined. Are those from within grains while those with large D and D' bands contain areas with a high grain boundary density?

Response:
We attempted to obtain all our measurements within grains. Therefore, we do not expect to be observing an effect from a variable grain boundary density.

Reply to Response:

Similarly to my comments above, a convincing micrograph may enhance the manuscript. The Raman microscope seems to have a normal optical system, so a light micrograph where grains/boundaries in an analysed area would be recognisable could be a good addition to the manuscript. The authors state (L200ff) that it might have been possible that some undeformed grains might haven been accidentally measured through fractures in the surface. A nice micrograph might be able to explain why fractures could accidentally be overlooked but grain boundaries be clearly identified.

I think the discussion about the applicability of the RSCM thermometer correction and the actual strain dependency should be conducted very carefully. An estimate on the strain within the deforming layer (e.g. via the thickness of the deforming layer, providing an upper estimate if it is assumed that all/most deformation is realised within those layers) in comparison to the minimum strain estimate derived from the bulk sample (if strain is correctly derived) may provide a more extensive explanation under which assumptions a "strain-correction" could realistically be applied.

Response 2: Here we provide a screen capture as an example of the areas we have been measuring with the Raman microspectrometer.

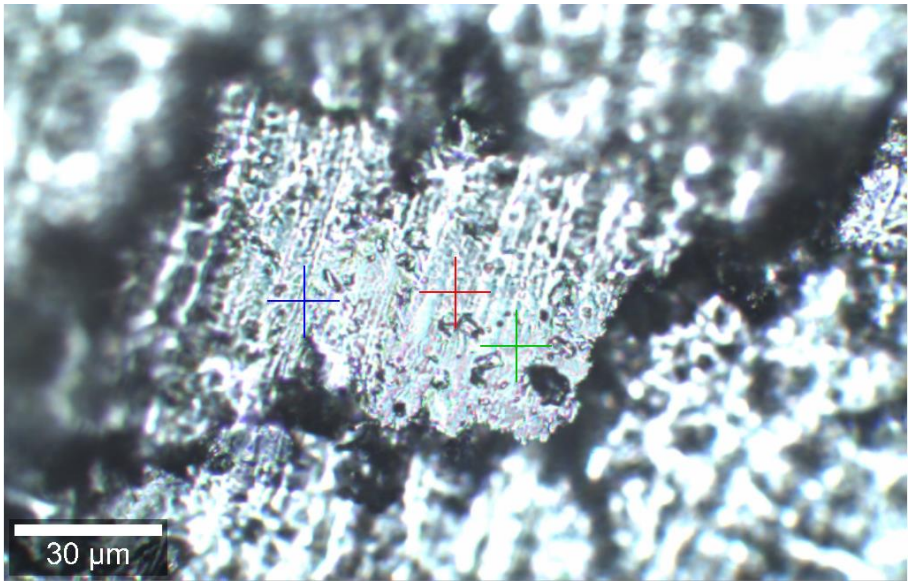

The manuscript and the reader would benefit from some definitions: crystallinity (vs structural ordering for example), interpretation of the peaks/bands in the Raman spectrum, (G being sp2 activation, D1 most likely to intraplane defects and D2 to out-of plane defects, sp3 defects ...) should be introduced and defined. Why are sliding velocity, slip rate, shear velocity are all used synonymously? The figures regarding the microstructural description might benefit from a better resolution since some feature referred to in the text cannot be seen in the figures (comments below).

Minor comments on the manuscript (l=line):
l 41:friction coefficient
Corrected. Now in line 43.

l 52: no "or"
Removed. Now in line 55.

l 54:160 m are maximum grain size?
Yes, 160 microns is the maximum grain size. This is now clarified in the text in line 57.

l 54: annealed instead of "cooked"?
Replaced. Now in line 57

l 85: Please introduce G,D1,D2
The information has been added in lines 89-90.

l 102: coefficient (please also correct that in the figures if you prefer to stay with friction coefficients instead of shear stress)
Thanks for the comment. This has been accordingly corrected throughout the manuscript.

l 103: coefficient
Added. Now in line 113.

l107: Plots ofat all slip rates ..: I do not see the gradual decrease of peak (numbers, if I'm not mistaken are 0.43, 0.43, 0.41, so I wouldn't call this a gradual decrease)
Thank you for the comment. The text is now modified accordingly (lines 119-120).

l 108 slip rates...shear velocity: is there any difference? Elsewhere like in the tables there is slip rate,sliding velocity, why are they all used synonymously, please settle for one term.
The text has been modified. We now use 'sliding velocities' throughout the manuscript.

l 110:Where are values of μss are read off?
μss were read at the end of each experiment. This information is now added to the manuscript in line 119.

l 135: retained instead of produced
Replaced with 'collected'. Now in line 145.

l 137: varies
Corrected. Now in line 147.

l140: high-pressure experiments: should be high normal stress experiments
Corrected. Now in line 150.

l 152: fractures with random orientation compared to the slip direction: I can't see those
These fractures are cross-cutting the documented slikenslides. See figure 4a.

l 155:...well-compacted layer
Corrected.

Fig 4c: hard to see in the Figure what is described in the text
The figure has been modified.

l156: "randomly oriented ... Fig 4d": Is that actually confirmed or just based on visual impression
We interpret these from our microstructural observations.

l 158: "weak fabric development (Fig. 4e)" I can't see this in the figure
We refer to the layer comprised of aligned graphite grains. On the figure it is marked with an arrow, labelled as 'foliation'.

l 159:"filled with smaller graphite grains...Fig 4f": also here, it is hard to see, I hope a better resolution of the image and some arrows may help
The figure has been modified.

l 176: "more efficient reorientation"What should that be, rotation per time, alignment after strain...?
We refer to previous interpretations by Morrow et al. (2000) that attribute the initial μpeak to the work involved in rotating the graphite grains with their (001) planes sub-parallel to the shear surfaces. This concept is introduced in the previous paragraph in lines 187-192.

l 178: This clear trend is not so clear to me.
The text has been modified accordingly.

l 180: "partial frictional heating": What should that be?
‘partial’ has been removed from the text for better clarity (line 197). Oohashi et al (2011) documented graphitization of carbonaceous material during high-velocity shear experiments due to frictional heating.

l 183 ff:The relation of compaction (volume change), thinning and the apparent dependency of"shear strain" on normal stress and displacement rate should be reconsidered, given
that no suitable measure for strain is used
We have previously justified our estimates of shear strain and we have additionally calculated total frictional work as it was suggested by reviewer 2. We hope this revised version of the manuscript will satisfy the reviewer.

l 188: replace high-pressure with high normal stress
Replaced. Now in line 205.

l 207: "stable mineral" from the thermodynamic point of view it is the stable mineral, so please explain your definition of "stable".
By ‘stable’ we mean that graphite crystallinity is known to increase with increase in temperature, and to remain unaffected by retrograde metamorphism (Buseck and Beyssac, 2014). This concept was introduced in the introduction in lines 27-30. For better clarity a reference is now added to the text in line 236.

l 291-223: There is a mixture of lithostatic pressure and normal stress: Any effect that is observed at higher normal stress does not mean there is a "significant effect of lithostatic pressure". Normal stress is not equivalent to confining/lithostatic pressure.
We now say ‘… it can be exposed to different lithostatic pressures, and hence different normal stresses ...’ (lines 249) because normal stress (both in nature or experiments) results from a lithostatic pressure and a differential stress.

l 234: "... microstructural observations provide some indications of the deformation processes..." These observations could be enhanced!
We have enhanced our discussion of microstructural observations. In addition, TEM analyses were also performed. (lines 264-274)

l 239: "plastic mechanisms" Such as?
We refer to any mechanisms that are likely to operate at higher temperatures and confining pressures than the ones implemented during our experiments.

l 240: "plastic deformation"
What should that be in contrast to the presented experiments where a gouge seems to flow by a rate independent mechanism?
We refer to deformation that takes place at higher temperatures and pressures than the ones implemented in our experiments (line 277).

l 244: "crystallographic structure ..." This seems to be a speculation neglecting a grain size effect.
We have clarified in the discussion that we collected our Raman spectra (mainly) from intragranular areas. Any occasional measurements along grain boundaries are unlikely to affect the overall analysis.

l 262ff: Any fit should consider the measure of strain as the independent variable, not as shown and calculated as the dependent one. Independent from that, (1) is not correct.
We have modified our plot and introduced new equation (line 302)

l 273: "We observe a trend..."So it appear there is an increasing thinning which however needs not to translate into an increased shear strain.
We take into account the sample thinning with increasing displacement and based on this relationship we calculate shear strain at equivalent record numbers.

l350: "approximate average crystallinity": What should that be?
We agree that 'approximate average crystallinity' is a bit confusing. We now say 'average crystallinity'(line 431).

Figures and Tables:
Table 1 and table 2 are mostly redundant and differ just by 1 column.
We acknowledge that the tables are very similar to each other. However, in table 2 the experiments are ordered in respect to increasing shear strain (rather than experiemental conditions) to emphasize the relationship between shear strain and R2.

Figure 1 It would be nice to use identical colors in (c) and (d) representing the displacement. Y-axis should read friction coefficient.
We have chosen to keep consistency with the plots in a and b instead. Meaning that exp. 1 and 5 have identical colours in all plots. Y-axis has been changed to 'friction coefficient'.

Figure 4 could strongly benefit from some images that more clearly show what is described in the text.
Thank you for the comment. We have modified the figure.

Supplementary material: If "int" stands for intensity and "pos" for wavenumber, it seems like the column headers are misplaced.
We are grateful for noticing this mistake. The supplementary material has been corrected.

Interactive comment on "Structural Disorder of Graphite and Implications for Graphite Thermometry" by Martina Kirilova et al.

O. Kiyokazu (Referee)
oohashik@yamaguchi-u.ac.jp

Received and published: 22 September 2017

This manuscript describes the effect of shearing on crystallinity of graphite by conducting biaxial friction experiments for powder of highly-crystalized graphite and micro- Raman analysis of the recovered sample. The manuscript documents systematic increase of crystallinity index, R2 value, which is widely used to determine paleomaximum temperature of metamorphic rocks, with increasing applied shear strain. Recently, much attention has been given to carbonaceous materials (including graphite) in and around a fault zone because of its utilities as a heat anomaly detector, displacement indicator, and lubricating agent of fault. However, crystallographic changes of graphite, especially in relation to the fault activities, are not well understood except for the effect of temperature alone. The objective of the manuscript is straightforward and their results seem sound. However, I found that some additional information and data are required and also there is room for further discussion and improvement. Hence I recommend accepting it with minor revisions.

General comments
Reviewer`s comment:
(1) The discussion about R2 and "shear strain" The main conclusion of this manuscript is R2 value of graphite increases (which implies decrease of crystallinity) with increasing applied "shear strain". However, "shear strain" you calculated corresponds to "bulk shear strain", and the bulk shear strain and microscopic shear strain which exactly concentrated into the narrow slip zone is quite different. Degree of compaction may differ depends on normal stress applied, hence the "bulk shear strain" reflects not only shearing but also compaction. Also, I would suspect thinning due to leakage of the gouge took place under 25 MPa experiments, especially for slip rate of 100 μm/s (Exp.10). All these issues make it difficult to extract an effect of shearing on the increments of R2 value. To solve this problem, I would suggest using total frictional work (shear stress*displacement) in addition to shear strain, and to discuss its relationship to R2 value.

Response:

This issue was also noted by another referee and we have documented our response to both comments in the other response to review. We agree that the measured bulk shear strain is most probably significantly lower than the shear strain accumulated only within the thin shear surfaces. However, we expect the shear strain variations within these surfaces to be linearly correlated with the measured bulk shear strain within a sample, but we recognise and acknowledge that we are only able to calculate a 'rough approximation' from our experimental data. In addition, we have now calculated frictional work as you suggested (Table 2 and Fig. 3b).

Reviewer`s comment:
(2) The relationship between R2 value and graphite "crystallnity" As another referee also mentioned, D bands (and R2 value) reflect amount of grain boundary (edge of grapheme sheet) in addition to intracrystalline defects, so determining which process is dominant in your setting becomes another problem to be addressed.

Response:
As we reported in a previous referee`s response, we attempted to avoid grain boundaries as much as possible, which was easily done due to the fact that the laser spot size (412 nm) was much smaller than the graphite grains in our samples (>10 microns, fig 4b). We acknowledge that some of the spectra may have been affected by an increase in the grain boundary density, however occasional measurements of this sort are unlikely to affect the average R2 per sample. Thus, we believe that the detected increase in D bands in our experimental data reflects disorder of the internal structure of graphite rather than grain size reduction. Nevertheless, a discussion addressing this topic is added in lines 225-233.

I could faintly see very small platelets of graphite (< 1μm) in your photograph (Figure 4e), but damages during shin-section making also make this kind of roughness. I think it is better to provide high-resolution SEM images of the slip surface if you could not make good thin section.

Response:
(1) We collected Raman spectra directly from the top of the sheared graphite gouges (referred to as shiny surfaces in the manuscript) to avoid damage induced during thin section making (the thin sections were made from other parts of the preserved experimental samples). High resolution SEM images of these surfaces (Fig. 4a and b) were also collected directly from the tops of the layers (labelled as XY sections in the manuscript).
(2) We imaged the zone underlying the shiny surfaces by cutting thin sections perpendicular to them. Thus, the small platelets of graphite (< 1μm) in Figure 4e, that you refer to, might have been affected by sample preparation. However, Raman spectra were not obtained from these samples, and thus the reported D bands do not reflect any damage induced during thin section making.

On the other hand, I think you should mention that the friction still remains low and stable if you applied shear strain >40. This feature may suggest the graphite on the slip surface still maintain its crystal perfection. In that sense, increments of R2 value of sheared graphite attributable mainly to grain size reduction but not amorphization.

Response:
Friction coefficients remain low and stable throughout all experiments. This is reflected in Fig. 1 and in lines 185-186. Our microstructural data clearly indicate partial structural disorder of the graphite structure, so we don't think that the reduction in the Raman spectra can be reasonably attributed just to grain size reduction. Also, please note there is no evidence of complete amorphization – graphite in all experiments remains crystalline even though significant defects in the graphite structure were introduced.

Specific comments:

Reviewer`s comment:
Line 46; I would happy if you add Oohashi et al. (2013, JGR) in the reference.
Response: The citation has been added into the reference list (in lines 378-380). Thank you for reminding us to properly acknowledge this excellent previous study.

Reviewer`s comment:
Line 60; I think initial thickness of gouge layer varies depends on applied normal stress if you put same weight of graphite powder for each experiments (becomes thinner under high normal

stress). Did you change amount of graphite for normal stress of 5 MPa and 25 MPa to ensure to form exactly the same 3-mm thickness? This question is arises from why large shear strain is calculated from the experiments under 25 MPa normal stress (off course, I understand your explanation about compaction). Additionally, I would suspect thinning due to leakage of the gouge took place under 25 MPa experiments, especially for slip rate of 100 µm/s (Exp.10) because the gouge thickness seems to became less than half of the initial thickness.
Response: The mass of graphite was not changed throughout the various experiments and hence we acknowledge the effect of normal stresses on the attained shear strain in lines 190-192 (as you have also noted in your comment). Your concern about potential leakage of gouge material during Exp. 10 is based on the dramatic layer thinning recorded at the end of this experiment. However, figure 1b clearly shows a linear trend of increase in shear strain (based on layer thinning) with increase of sliding velocities in the experiments under normal stresses of 25 MPa (ranging from 21,45 through 31.86 to 46,77 in Exp. 8, 9 and 10 respectively). Therefore, we believe that leakage of gouge material is unlikely to have affected the measured layer thickness.

Reviewer`s comment:
Line 109-110; The authors documented µss does not depend on slip rates, and it remains constant for all experiments. However, I see clear relationship between µ at d=14-20 mm and slip rates; µ decreases with decreasing slip rates for σn=5 MPa, and µ decreases with increasing slip rates for σn=25 MPa.
Response: Dependence of µss on slip rates is not suggested by our data (Table 1). Instead we observe slight variations in 2 of the performed experiments (Exp. 4 and 10). This is reflected in the manuscript in lines 119-120.

Reviewer`s comment:
Line 141-143; The authors explain graphite crystalinity decreases with increasing slip rates for samples sheared under _n=25 MPa, and no slip rates dependence is found for samples sheared under _n=5 MPa. However, as you concluded, increase of R2 value can be attributed to applied shear strain but not to slip rates. I think you can not discuss direct relationship between R2 value and slip rates unless you conduct various slip-rates experiments at exactly the same shear strain.
Response: In lines 151-153, we simply compare the observed decrease in graphite crystallinity with the conditions of the experiments but do not imply direct relationship between R2 and slip rates. Then (lines 153-154), we conclude that ‘graphite appears as most disordered in the experiments where the highest shear strain was achieved’.

Reviewer`s comment:
Line 181; I would suggest referring Di Toro et al. (2011, Nature) instead of Nakatani (2001).
Response: Thank you for the suggestion. The reference is now updated. (line 198)

Reviewer`s comment:
Table 2 and Figure 3 Please add errors and error bars for R2 value.
Response: Error estimates are now added in table 2 and line 432.

Hope this helps,
Kiyokazu Oohashi, Yamaguchi University, Japan

Structural Disorder of Graphite and Implications for Graphite Thermometry

Martina Kirilova[1], Virginia Toy[1], Jeremy S. Rooney[2], Carolina Giorgetti[3], Keith C. Gordon[2], Cristiano Collettini[3], Toru Takeshita[4]

[1] Department of Geology, University of Otago, PO Box 56, Dunedin 9054, New Zealand

[2] Department of Chemistry, University of Otago, PO Box 56, Dunedin 9054, New Zealand

[3] Dipartimento di Scienze della Terra, Università degli Studi La Sapienza, Rome, Italy

[4] Faculty of Science, Earth and Planetary Sciences, Hokkaido University, Sapporo, Japan.

Correspondence to: Martina Kirilova (martina.a.kirilova@gmail.com)

Key Points:

graphite, disorder, thermometry, Raman

Abstract

Graphitization, or the progressive maturation of carbonaceous material, is considered an irreversible process. Thus, the degree of graphite crystallinity has been calibrated as an indicator of the peak metamorphic temperatures experienced by the host rocks. However, discrepancies between temperatures indicated by graphite crystallinity versus other thermometers have been documented in deformed rocks. To examine the possibility of mechanical modifications of graphite structure and the potential impacts on graphite 'thermometry' we performed laboratory deformation experiments. We sheared highly crystalline graphite powder at normal stresses of 5 and 25 MPa and aseismic ~~slow sliding~~ velocities of 1 µm/s, 10 µm/s and 100 µm/s. The degree of graphite crystallinity both in the starting and resulting materials was analyzed by Raman microspectroscopy. Our results demonstrate consistent decrease of graphite crystallinity with increasing shear strain. Microstructural observations show that brittle processes caused the documented structural disorder of graphite. We conclude that the calibrated graphite 'thermometer' is ambiguous in active tectonic settings and we suggest that a calibration that accounts for shear strain is needed.

1. Introduction

Organic matter, preserved in sedimentary rocks, can be transformed into crystalline graphite due to structural and compositional changes during diagenesis and metamorphism, a process known as graphitization (Bonijoly et al., 1982; Wopenka and Pasteris, 1993; Beyssac et al., 2002a; Buseck and Beyssac, 2014; etc.). Graphitization is thought to be an irreversible process and graphite is known to remain stable to the highest temperatures of granulite facies and the highest pressures of coesite-eclogite facies (Buseck and Beyssac, 2014). It is generally accepted that the degree of graphite crystallinity, or its structural order, is determined mainly by the maximum temperature conditions experienced by the host rocks, whereas lithostatic pressure and shear strain are considered to have only minor influence on graphitization (Bonijoly et al., 1982; Wopenka and Pasteris, 1993; Bustin et al, 1995). Therefore, graphite crystallinity has been calibrated as an indicator of the peak temperatures reached during progressive metamorphism (Beyssac et al., 2002a; Reitmeijer and McKinnon, 1985). However, in strained rocks discrepancies between temperatures indicated by the crystallinity of graphite vs. other thermometers have been reported (Barzoi, 2015; Nakamura et al., 2015; Kirilova et al., in press). Thus, numerous authors have speculated that tectonic deformation results in graphite structural modifications that challenge the validity of the existing graphite thermometers (Large et al., 1994; Bustin et al, 1995; Crespo et al., 2006; Barzoi, 2015; Nakamura et al., 2015).

Furthermore, graphite occurrence and enrichment have been documented in several fault zones in the world, e. g. the Alpine Fault zone, New Zealand (Kirilova, et al., in press), the Hidaka metamorphic belt, Hokkaido, Japan (Nakamura et al., 2015), the Atotsugawa fault system, Japan (Oohashi, et al., 2012), the Tanakura Tectonic Line, Japan (Oohashi et al., 2011), the Err nappe detachment fault, Switzerland (Manatschal, 1999), and the KTB borehole, Germany (Zulauf et al., 1990). In these intensely deformed rocks its presence is of particular interest because its low friction ~~at~~ coefficient of $\mu \sim 0.1$ (Morrow et al., 2000) allows graphite to act as a natural solid lubricant (Savage, 1948). The mechanical behavior of graphite has been broadly investigated in both natural and experimental specimens, where it manifests with the lowest μ among sheet structure minerals (Moore and Lockner, 2004; Oohashi et al., 2011, 2013; Rutter, et al., 2013; Kuo et al., 2014, etc.) confirming it could have a significant impact on fault mechanics. It has been experimentally proven that even a small fraction of graphite ~~has~~ can have a disproportionally large effect on frictional strength ~~due to concentration of smeared~~where graphite is concentrated by smearing into interlinked layers (Rutter, et al., 2013).

However, structural changes in crystalline graphite caused by tectonic deformation have not yet been ~~explained until now~~systematically explored. To examine this aspect and to investigate the potential impacts of structural disordering of graphite on the graphite 'thermometer', we have carried out laboratory deformation experiments on highly crystalline graphite powder.

2. Experimental methods

2.1 Sample description

As a starting material in the current study we used synthetic (~~or~~ commercially synthesized) graphitic carbon to avoid complexities arising from variable degree of crystallinity in natural carbon materials. Initially, the material was crushed to maximum grain size of 160 μm in a RockLabs Swing (TEMA) mill. The resulting fine graphitic powder was ~~'cooked'~~annealed at 700˚C for two hours in a Lindberg Blue M Muffle Furnace to achieve full graphitization, which is known to occur at this temperature in the absence of other variations in physical conditions (Buseck and Beyssac, 2014). This was used as the starting material for the deformation experiments.

2.2 Experimental procedure

In total, 10 deformation experiments were performed at room temperature and room humidity in the Brittle Rock deformAtion Versatile Apparatus BRAVA (Collettini et al., 2014), at INGV, Rome. For each experiment two 3-mm thick layers of synthetic graphite gouges were placed in between three grooved forcing blocks in a double-direct shear configuration (e.g. Dieterich, 1972). The two side blocks are held stationary, and the central forcing block is driven downward causing shear to occur within the graphite gouge layers. Normal stress is applied by the horizontal piston in load-feedback control mode and shear displacement accomplished by the vertical piston in displacement-feedback control mode. Forces are measured with stainless steel load cells (± 0.03 kN) and displacements are measured with LVDTs (± 0.1 μm) attached to each piston. Experiments have been conducted at normal stresses of 5 MPa or 25 MPa and aseismic sliding velocities of 1 μm/s, 10 μm/s and 100 μm/s. The experiments were carried out to total displacements of 20 mm. In addition, some experiments were stopped at 5 mm and 10 mm and the specimens were then recovered to reveal graphite structural changes that took place during different amounts of total deformation. The coefficient of friction (μ) was calculated as the ratio of measured shear load to measured normal load ($\mu = \tau / \sigma_n$, where τ is shear stress and σ_n is effective normal stress). The average shear strain within the layer was calculated by dividing shear displacement increments by the measured layer thickness and summing. The displacement values of the vertical and horizontal load points were corrected for the elastic stretch of each load frame, taking into account that the machine stiffness is 1283 kN/mm on the horizontal axis and 928.5 kN/mm on the vertical axis. In addition, we calculated total frictional work for each experiment as a function of shear stress integrated over the total displacement (Beeler, 2007).

2.3 Raman microspectroscopy

The degree of graphite crystallinity was measured by an Alpha 300R+ confocal Raman microscope (WITec, Ulm, Germany) with a 532 nm laser (Coherent, Santa Clara, California), located at the Department of Chemistry, University of Otago, New Zealand. The laser (3.0 mW) was focused on the samples with a 50× Zeiss objective. The scattered light was dispersed with a 1200 g/mm grating. The combination of the 50× objective and 532 nm laser wavelength produced a laser spot size of approximately 412 nm in diameter. The integration time of each spectrum was 2 seconds with 50 co-additions (100 seconds in total). The spectra were calibrated using the Raman band from a silicon wafer prior to each set of measurements.

The collected spectra were pre-processed in GRAMS AI 9.1 (Thermo Fisher Scientific Inc.), where cosmic spikes were removed and a multi-point linear baseline offset was performed. This was followed by peak fitting three Lorentzian-Gaussian functions to each spectrum with a linear baseline over 1000 - 1700 cm^{-1}. For each spectrum, the area ratio was calculated ($R2 = A_{D1} / (A_G + A_{D1} + A_{D2})$, where A*i* is the= area of the *i*th peak, G band is the main high frequency band of graphite, D1 and D2 bands are defect bands observed in the first order Raman spectrum of graphite) (Wopenka and Pasteris, 1993; Beyssac et al.., 2002a).

2.4 Scanning electron microscopy

Microstructural analyses of the graphite gouge recovered from the biaxial apparatus were carried out using a scanning electron microscope (SEM). Some SEM images were acquired from the shiny surfaces of the graphite layers that had been parallel to the center and or side forcing blocks (Y-Z sections), with a Zeiss Sigma field emission scanning electron microscope (VP FEG SEM) at the Otago Centre for Electron Microscopy (OCEM), University of Otago, New Zealand. The instrument was operated in variable pressure mode (VP) at 15 kV using a working distance (WD) of 7 – 8 mm and a VPSE (VP-mode secondary electrons) detector. In addition, polished thin sections cut perpendicular to the surface of contact with the center and side forcing blocks (X-Z sections) were imaged on a JEOL JSM-6510 SEM at the University of Potsdam, Germany, where high-resolution secondary electron images were collected at 20 kV and a WD of 10 mm.

2.5 Transmission electron microscopy

Transmission electron microscopy (TEM) was used for detailed microstructural characterization of the shiny surfaces. High-resolution TEM images were collected by using a JEM-2010 electron microscope, located at the University of Hokkaido, Sapporo, Japan. The instrument was operated at 200 kV with LaB6 filament. TEM foils (with size of 12 x 5 µm and thickness of 1 µm) milled by FIB perpendicular to the shiny surface (X-Z section) were placed on a carbon coated film, and examined by using dual-axis tilting holder.

3. Results

3.1 Mechanical data

Our experiments allowed us to investigate graphite mechanical behavior and structural modifications under various sliding velocities, normal stresses and shear strain. These conditions are summarized in Table 1.

3.1.1 Friction variations

Over several mm of displacement, the friction coefficient shows a similar evolution trend in all experiments. On a plot of friction coefficient vs. displacement (Fig. 1a), the friction coefficient (μ) delineates a curve characterized by a rapid increase to an initial peak friction coefficient (μ_{peak}), followed by a subsequent exponential decay towards a steady-state friction coefficient (μ_{ss}) over a slip weakening distance. The shapes of the friction-displacement curves vary with the normal stress applied and are steeper for the experiments conducted at 25 MPa than the ones at 5 MPa (Fig. 1a) i.e. the displacement required to achieve steady-state decreases at higher normal stress. In addition, the values of both μ_{peak} and μ_{ss} (Fig. 1a; Table 1) are significantly lower in the experiments at 25 MPa (μ_{peak} = ~0.4; μ_{ss} = ~ 0.1) than in the experiments at 5 MPa (μ_{peak} = ~0.5; μ_{ss} = ~ 0.2) (where μ_{ss} values were read at the end of each experiment). Plots of μ at all sliding velocities (Fig. 1a) show subtle variations in μ_{peak} and μ_{ss} with change of the applied sliding velocities (Fig. 1a; Table 1).

~~Plots of μ at all slip rates (Fig. 1a) indicate a gradual decrease of μ_{peak} with increasing shear velocity at high normal stress (Table 1). In the experiments at 5 MPa subtle variations in μ_{peak} also occur but a velocity related trend is not observed. μ_{ss} does not depend in any experiment on slip rates, and μ_{ss} remains constant for experiments at both low and high normal stress (Fig. 1a; Table 1).~~

3.1.2 Shear strain variations

Plots of friction coefficient vs. shear strain (Fig. 1b) show significant variations in shear strain attained over equivalent sliding displacements. The estimated shear strain values are a geometric consequence of different thickness changes. Consideration of the shear strain at equivalent sliding velocities but different normal stresses demonstrates that shear strains achieved during the 5 MPa experiments are approximately half of those at 25 MPa (Fig. 1b; Table 1). In addition, the experiments at 25 MPa demonstrate a dramatic increase in shear strain with increasing slip velocity (Fig. 1b; Table 1), whereas at low normal stress we do not observe any systematic variations associated with changes in sliding velocities (Fig. 1b, c and d). Fig. 1c and d show the experiments at low shear strain used to characterize graphite structural changes in the early stages of deformation (Table 1).

3.2 Graphite crystallinity

All the experiments resulted in the development of shiny smooth surfaces with gentle slickenlines (macroscopic fine grooves, parallel to the slip direction as defined by Toy et al., in press). Raman spectra obtained on the top of these surfaces, that had accommodated most of the induced deformation, are compared to Raman spectra from the starting material to identify the effects of mechanical deformation on graphite crystallinity.

Raman data from 20 spectra per sample are presented in Supplementary material 1 (S1). Representative spectra for each sample are illustrated in Fig. 2, which shows spectra displaying the least (left column) and the most (right column) disordered graphite within a sample (i.e. lowest and highest R2 values respectively). Spectra that were typical of the average for each sample are also presented (middle column). Experiments 3 and 7 were stopped at only 5 mm displacement and resulted in extremely fragile deformed surfaces, which were unable to be extracted without them breaking into pieces too small to obtain spectra from. Thus, graphite crystallinity was not measured in these experiments.

All the acquired spectra show typical G, D1 and D2 bands, respectively at ~1580 cm^{-1}, ~1350 cm^{-1} and ~1620 cm^{-1} (S1). The degree of graphite crystallinity in each sample could thus be calculated by using the area ratio R2 (Fig. 2; S1). Raman spectra collected from the starting material show R2 values ranging from 0 to 0.327 (Fig. 2), corresponding respectively to fully crystalline and highly organized graphite. Spectra acquired from the deformed surfaces show higher R2 values (Fig. 2; S1). The most crystalline graphite with R2=0.330 was ~~produced~~ collected in Exp. 2 (Fig. 2) while the most disordered graphite with R2=0.661 resulted from Exp. 10 (Fig. 2).

As graphite crystallinity varies~~y~~ within a sample (Fig. 2; S1), we examine average R2 values for each one and compare them with applied normal stress, sliding velocity, ~~and~~ shear strain, and total frictional work (Table 2). The starting material has average $R2_{\text{pre-shear graphite}}$ = 0.173, whereas all deformed samples have higher average R2 values (Table 2). Analyzing the average R2 values for deformed samples reveals that graphite is more disordered in the high ~~pressure~~ normal stress experiments (Table 2) than in the experiments at 5 MPa. Furthermore, in the experiments at 25 MPa the average graphite crystallinity decreases with increasing sliding velocities (Table 2). In contrast, at low normal stress, we do not observe any dependence of the degree of graphite crystallinity on the applied sliding velocities (Table 2). Overall graphite appears as most disordered in the experiments where the highest shear strain was achieved (Table 2). The~~is~~ relationship between average R2 and shear strain is illustrated in Fig. 3a by fitting a power function with a correlation coefficient R^2 = 0.95. Fitting a power function to average R2 and total frictional force showed a consistent correlation (Fig. 3b). The experiments 2 and 6 at low normal stress, which were stopped at 10 mm displacement and accommodated the least amount of shear strain, contain the least disordered graphite (Fig. 3; Table 2).

3.3 Microstructural characteristics

3.3.1 Scanning electron microscopy (SEM)

Similar microstructural features were observed in all the deformed samples. SEM images obtained from the sample deformed during experiment 8 are presented to demonstrate our observations (Fig. 4).

These high-resolution images in Y-Z sections reveal that the shiny surfaces are decorated by closely spaced (from < 5 to 10 micrometers) slickenlines (Fig. 4a), on top of a smooth continuous layer. In places, the continuity of this layer is interrupted by fine (~1 to 2 micrometers in width) fractures (Fig. 4a), with random orientation compared to the slip direction. Occasionally, the deformed surface appears as completely disrupted, ~~comprising of platy graphite~~and is decorated with smaller graphite grains from 10 to 50 micrometers in size, oriented nearly parallel to the shear direction (Fig. 4b). In X-Z sections this highly deformed surface is observed as a thin slip-localized zone, composed of well-compacted layer of aligned graphite grains (Fig. 4c). This localized shear surface is underlain by a zone of randomly oriented, inequigranular, irregular graphite grains (Fig. 4d). In places, most of the graphite grains are aligned with their basal (001) planes parallel to the slip direction, and form compacted layers, defining a weakly-developed fabric ~~development~~ (Fig. 4e). There has been some dilation along these cleavage planes, and the spaces thus created are filled with smaller graphite grains with their (001) planes sub-perpendicular to the shear direction (Fig. 4e). Locally, intensely fractured grains are also observed (Fig. 4f).

3.3.2 Transmission electron microscopy (TEM)

TEM was used to examine the microstructure of the material that makes up the shiny surfaces (Fig. 4c). TEM analyses were performed on foils cut perpendicular to this surface. Fig. 5 shows characteristic TEM images obtained from the sample recovered from experiment 8.

Graphite grains in this well-compacted layer have basal planes predominantly aligned with the shear plane, as were observed in SEM images. However, adjacent grains show slightly different orientations (Fig. 5a). In addition, kink folded graphite grains are observed in multiple locations in the foils (Fig. 5b, c), which yields a 'wavy layering' at a small angle to the shear direction (Fig. 5b). In isolated areas, there are also some smaller grain fragments with random orientation (Fig. 5d).

4. Discussion

4.1 Mechanical behavior

Graphite in our experiments shows mechanical behavior consistent with other mechanical studies of pure graphite gouges. Our results display low μ_{ss} values (from ~0.1 to ~0.2; Table 1) as did the low-pressure deformation experiments of

carbonaceous material performed by Morrow et al. (2000), Moore and Lockner (2004), Oohashi et al. (2011, 2013), Kuo et al. (2014), and Rutter et al. (2013). The low frictional strength of graphite is well known and has been attributed to its sheet structure composed of covalently bonded carbon atoms held together only by van der Waals forces. These weak interlayer bonds along (001) planes are easily broken during shear (Moore and Lockner, 2004; Rutter, et al., 2013). Initial μ_{peak} followed by strain weakening during deformation experiments of graphite gouges has been previously explained with the work involved in rotating the grains with their (001) planes sub-parallel to the shear surfaces, which puts them in the optimal position for shearing along the weak interlayer bonds (Morrow et al., 2000; Moore and Lockner, 2004; Rutter, et al., 2013).

Controversially, Oohashi et al. (2011) reported an absence of μ_{peak} in pure graphite gouges sheared at $\leq$ 2 MPa with sliding velocities of 1.3 m/s. Instead shearing started and continued at a similar μ throughout their experiments. ~~Our data indicate that μ_{peak} tends to increase with decreasing normal stresses (see experiments at 25 MPa vs. 5 MPa: Fig. 1a; Table 1), therefore, we attribute the discrepancies in graphite frictional strength to the effect of sliding velocity on graphite friction.~~ We hypothesize that higher velocities result in more efficient reorientation of graphite grains, and therefore, μ_{peak} is not present in experiments carried out at seismic rates. ~~This hypothesis is also consistent with the observations from our experiments at 25 MPa that clearly indicate a trend of decreasing μ_{peak} with increasing sliding velocity (Fig. 1a, b; Table 1).~~ We also acknowledge that the imposed velocities in the experiments by Oohashi et al. (2011) were substantially different to ours, and shearing at those seismic rates may cause ~~partial~~ frictional heating. Therefore, graphite frictional strength in their experiments may be related to thermally-activated weakening mechanisms (~~Nakatani, 2001~~Di Toro et al., 2011) that are only significant at these high velocities.

We also observed shear strain variations in the various samples (Fig. 1b, c and d) that are systematically related to the conditions of the experiments. The calculated shear strain (or the ratio of shear displacement to measured layer thickness) is ~~linearly~~ directly dependent on the applied normal stress, and shear strains are significantly higher in the experiments performed at 25 MPa than the ones at 5 MPa due to better compaction and thinning of the sheared graphite gouges. Furthermore, ~~slip rates~~sliding velocities also play a role in the accommodated total shear strain, and shear strain increases with increase in the applied sliding velocities but only in the high ~~pressure~~ normal stress experiments (Fig. 1b). As we previously suggested, higher velocities may result in more efficient reorganization of graphite grains, and thus further progressive thinning of the graphite gouges occurred. However, we cannot explain the absence of similar trend at the 5 MPa experiments by our results. There are too few of these relationships to fully characterize the effect of sliding velocity on shear strain accumulation in graphite gouges, and more mechanical data of this sort need to be collected in future.

4.2 Structural disorder of graphite

Our experimental study clearly demonstrates transformation of fully/highly crystalline graphite (with R2 ratios ranging from 0 to 0.327; Fig. 2; S1) into comparatively poorly organized graphitic carbon (with R2 ratios up to 0.661; Fig. 2; S1), which

indicates significant graphite disorder with increasing strain and total frictional work at the tested aseismic sliding velocities (Fig. 3). The estimated bulk shear strains (Table 1) are likely to be significantly lower than the shear strains accommodated within the thin shear surfaces. However, we expect the strain variations within these surfaces to be directly related to the measured bulk shear strains. Nevertheless, we refer to the above relationship as a rough approximation. We also acknowledge that the slickenlined surfaces that were produced experimentally contain some graphite that yield spectra comparable to those acquired from the starting material i.e. there is highly crystalline graphite that appears as unaffected by the deformation. However, at least some of these spectra are derived from undeformed graphite powder that underlies the shear surfaces and could not be entirely removed during sample preparation due to the fragile nature of the samples. It is also possible that some non-deformed graphite powder was accidently measured through the fractures that are cross-cutting the accumulated shear surfaces (Fig. 4a). But even if some graphite did not undergo mechanical modification during the experiments, the results overall validate that structural disorder of graphite can result from shear deformation subsequent to the graphitization process.

We evaluate the documented disorder of the crystal structure of graphite by analyzing variations in R2 ratios, which depend on the increase of defect bands (D1 and D2) in the Raman spectrum of graphite. This relationship is a well-known crystallinity index of graphite that shows the degree of maturity of the carbonaceous material (Wopenka and Pasteris, 1993; Beyssac et al., 2002a; etc.). Alternatively, it may reflect increase in the grain boundary density (Tunistra and Koening, 1970; Pimenta et al., 2007). However, we aimed to avoid grain boundaries during spectra acquisition, which was possible due to the laser spot size of 412 nm, which is much smaller than the graphite grains in our samples (>10 microns, Fig. 4b). We acknowledge that some of the spectra may have been accidentally obtained in close proximity to grain boundaries, however occasional measurements of this sort are unlikely to affect the average R2 per sample. Thus, we attribute the detected increase in D bands in our experimental data to disorder of the internal structure of graphite rather than grain size reduction.

Our findings contradict the paradigm that the degree of graphite crystallinity is determined by an irreversible maturation of carbonaceous material (Bonijoly et al., 1982; Wopenka and Pasteris, 1993; Beyssac et al., 2002a; Buseck and Beyssac, 2014). Therefore, graphite should not be considered as a stable mineral (Buseck and Beyssac, 2014), especially in active tectonic settings, where mechanical motions, such as fault creep, may cause disordering of the structure of carbonaceous material that formed during typical graphitization processes. Similar assumptions have been made on graphite in intensely deformed cataclasites (comprising crushed mylonitic chips floating in a fine-grained matrix) that is significantly disordered in comparison with graphite in the spatially associated mylonitic rocks (Kirilova et al, in press; Nakamura et al., 2015).

We have experimentally proven that shear strain can not only affect the final structural order of graphite but also manifests as a controlling parameter in the transformation process (Fig. 3a; Table 2). Previous authors have suspected that shear strain may play an important role for graphite modifications, and evidence for this has been found in graphite crystallinity

variations in natural samples from active fault zones (Kirilova et al, in press; Nakamura et al., 2015), and strained rocks in metamorphic terrains (Barzoi, 2015; Large et al., 1994). Thus, we conclude that the previously proposed model of progressive graphitization due to increase of temperature (Bonijoly et al., 1982) does not completely reflect the graphite formation mechanisms.

Furthermore, graphite can form or be transported at various depths by tectonic processes, and therefore, it can be exposed to different lithostatic pressures, and hence different normal stresses. We demonstrated that during shearing higher normal stress results in an increase of shear strain (Fig. 1b), and thus causes a higher degree of graphite disorder (Fig. 3a; Table 2). This outlines the significant effect of lithostatic pressure on graphite crystallinity that has been undervalued until now (Bonijoly et al., 1982; Wopenka and Pasteris, 1993; Bustin et al, 1995; Beyssac et al. 2002b). Previous experimental studies have identified initiation and enhancement of graphitization under pressure (i. e. increase in graphite crystallinity) but only at nanometer scale (Bonijoly et al., 1982; Beyssac et al., 2003). Nevertheless, we speculate pressure should be also considered as a factor that can determine the degree of graphite crystallinity during both graphitization and graphite structural modifications.

We have investigated the effects of shear strain and pressure on graphite crystallinity during shear deformation with aseismic velocities, using a starting material with uniform properties (i.e. highly crystalline graphite powder). In contrast, Kuo et al. (2014) and Oohashi et al. (2011) simulated fault motions in synthetic and natural carbonaceous material with variable degree of maturity at the start of the experiments (ranging from amorphous carbonaceous material to crystalline graphite). Both studies reported graphitization of carbonaceous material due to localized frictional heating rather than structural disordering. These experiments reveal the impact of seismic velocities on graphite structural order and the fact their findings differ so markedly from ours highlights the complexity of graphite transformations in fault zones.

Our microstructural observations provide some indications of the deformation processes that affected graphite structural order. The shiny slickenlined surfaces are composed of very fine-grained material visible as slip-localized zone on SEM images (Fig. 4d). Nanoscale observations reveal graphite grains within it occasionally form stacked kink-band structures, (Fig. 5b, c). This zone, which we assume accommodated most of the induced deformation, is underlined by a less deformed zone composed of larger graphite grains in a finer matrix that in places has developed as an anastomosing fabric, typical of creeping gouges (Fig. 4d). In rare places at SEM scale brittely fractured grains also occur (Fig. 4f and 5d). The interpreted structures suggest that brittle processes operated during shearing, and we conclude that these processes resulted in the structural disorder of graphite, manifested as changes in the Raman spectra. This interpretation is in agreement with the conditions of our experiments (i.e. shearing with aseismic velocities took place at room temperature conditions), that typically would not induce temperatures high enough for crystal plastic processes. Furthermore, the microstructures and the inferred processes are exactly the same as those observed by Nakamura et al. (2015) in the Hidaka metamorphic belt, Japan.

~~They reveal a thin slip localized zone (Fig. 4d), underlined by a less deformed zone with typical cataclastic fabric (random fabric (Fig. 4d), affected by occasional fractures (Fig. 4f)). These observations demonstrate that brittle processes operated during shearing and we infer these processes resulted in the structural disorder of graphite, manifested as changes in the Raman spectra.~~ However, crustal fault zones do not only accommodate brittle deformation~~;~~. ~~a~~At ~~`~~higher temperatures and~~,~~ confining pressures~~, and lower strain rates~~, localised shearing ~~may be accommodated~~can operate by plastic mechanisms (White et al., 1980). We hypothesize that graphite crystallinity ~~can~~ could also be influenced by plastic deformation, as was also suggested in previous studies by Large et al. (1994), Bustin et al. (1995), Barzoi et al. (2015). Investigating this hypothesis and identifying the exact effects of strain on graphite crystallinity during ductile deformation remain goals for future research.

4.3 Implications for graphite thermometry

The crystallographic structure of graphite measured by Raman spectroscopy has been applied as a thermometer that relies on progressive maturation of originally-organic carbonaceous material during diagenesis and metamorphism. Previous studies have focused on calibrating this thermometer. The current best calibration is described by the following equation T (ºC) = -445 * R2 + 641 ± 50 (Beyssac et al. 2002) by inferring a linear correlation between R2 ratio and peak metamorphic temperatures. However, this thermometer disregards the effects of mechanical modifications of the graphite structure, which this study has identified as having a substantial influence on graphite crystallinity in deformed rocks at sub-seismic velocities.

Our experiments demonstrate a shear strain-dependent increase of the R2 ratio of initially highly crystalline graphite powder due to brittle ~~shear~~ deformation (Fig. 3a; Table 2). In natural analogues, the pre-shear graphite would yield temperatures up to 641 ± 50 ºC (S1), which is the upper limit of the calibrated thermometer (Beyssac et al. 2002). Whereas, the sheared samples would indicate peak metamorphic temperatures as low as 347 ± 50 ºC (estimated from the most strained samples; S1). Thus, we experimentally prove that in active tectonic settings graphite thermometers may underestimate the peak metamorphic temperatures by < 300 ºC. In cataclasites from the Alpine Fault zone, New Zealand (Kirilova et al., in press) and fault zones of the Hidaka metamorphic belt, Japan (Nakamura, et al., 2015), the graphite thermometer yields temperature discrepancies of more than 100 ºC compared to temperature estimates derived both from the surrounding high-grade amphibolite facies mylonites and the lower grade equilibrium cataclastic phases (marked by chlorite alteration). Barzoi (2015) also described differences of ~ 150 ºC in graphite temperatures between strained and less strained low grade metamorphic rocks from Parang Mountains, South Carpathians.

We conclude that shear strain calibration of the current graphite thermometer is needed, and we propose an appropriate adjustment based on our dataset. Fig. 3a illustrates good correlation between the average R2 and the bulk shear strain measured within a sample, which can be described by the following equation (1):

$F(x) = 0.14017 * x^{0.30713} + 0.15629$ with a correlation coefficient $R^2 = 0.95$ (1)

where x = bulk shear strain.

However, a calibration of the existing graphite thermometer could be still insufficient to permit reliable temperature estimates in active tectonic settings because ~~of the variable~~both aseismic and seismic ~~slip rates~~sliding velocities are likely to be encountered in fault zones, resulting in structural disorder of graphite or graphitization (Oohashi et al., 2013) respectively. Furthermore, it can be challenging to estimate shear strain in natural samples, so a strain-calibrated graphite thermometer may be impossible to use in deformed rocks.

5. Conclusions

We have experimentally demonstrated that graphite crystallinity ~~is not irreversible~~can be reduced by deformation by performing shear deformation experiments at aseismic sliding velocities insufficient to generate appreciable frictional heat on graphite gouges composed of powdered highly-organized graphite. Our results clearly demonstrate significant decrease in graphite structural order, which is a function of the total shear strain attained during the various experiments. Microstructural data presented here reveal that this is a result of brittle processes. We also observed a trend of increasing shear strain within a sample with increase in the applied normal stresses and sliding velocities. This reveals the complexity of graphite structural modifications and highlights the significance of the various parameters that can affect the graphitization process. ~~Furthermore, o~~Our findings compromise the validity of the calibrated graphite thermometer ~~as~~ by showing they may underestimate the peak metamorphic temperatures in active tectonic settings. ~~Thus, w~~We ~~tentatively~~ further suggest a simple shear strain calibration of this thermometer.

Acknowledgments

The research was funded by the Department of Geology, University of Otago, New Zealand, and Rutherford Discovery Fellowship RDF-UOO0612 awarded to Virginia Toy. We also acknowledge the 'Tectonics and Structure of Zealandia' subcontract to the University of Otago by GNS Science (under contract C05X1702 to the New Zealand Ministry of Business, Innovation and Employment). We thank our colleagues Gemma Kerr and Brent Pooley for assistance in sample preparation, and Hamish Bowman for helping with data visualization. We also wish to express our gratitude to Laura Halliday for generously offering to perform grain size analysis on our samples at the Department of Geography, University of Otago, New Zealand. And last but not least, we thank Marco Scuderi for valuable discussions and assistance throughout the experimental procedures.

References

Barzoi, S. C.: Shear stress in the graphitization of carbonaceous matter during the low-grade metamorphism from the northern Parang Mountains (South Carpathians)—Implications to graphite geothermometry, International Journal of Coal Geology, 146, 179-187, 2015.

Beeler, N. M.: Laboratory-observed faulting in intrinsically and apparently weak materials: Strength, seismic coupling, dilatancy, and pore-fluid pressure, The Seismogenic Zone of Subduction Thrust Faults, pp.370-449, 2007.

Beyssac, O., Goffé, B., Chopin, C. and Rouzaud, J. N.: Raman spectra of carbonaceous material in metasediments: a new geothermometer, Journal of Metamorphic Geology 20.9: 859-871, 2002a.

Beyssac, O., Rouzaud, J. N., Goffé, B., Brunet, F., and Chopin, C.: Graphitization in a high-pressure, low-temperature metamorphic gradient: a Raman microspectroscopy and HRTEM study, Contributions to Mineralogy and Petrology, 143(1), 19-31, 2002b.

Beyssac, O., Brunet, F., Petitet, J. P., Goffé, B., and Rouzand, J. N.: Experimental study of the microtextural and structural transformations of carbonaceous materials under pressure and temperature, European Journal of Mineralogy, 15(6), 937-951, 2003.

Bonijoly, M., Oberlin, M. and Oberlin, A.: A possible mechanism for natural graphite formation, International Journal of Coal Geology, 1.4: 283-312, 1982.

Buseck, P. R. and Beyssac, O.: From organic matter to graphite: Graphitization, Elements, 10.6: 421-426, 2014.

Bustin, R. M., Ross, J. V., and Rouzaud, J. N.: Mechanisms of graphite formation from kerogen: experimental evidence, International Journal of Coal Geology, 28(1), 1-36, 1995.

Collettini, C., Di Stefano, G., Carpenter, B., Scarlato, P., Tesei, T., Mollo, S., Trippetta, F., Marone, C., Romeo, G. and Chiaraluce, L.: A novel and versatile apparatus for brittle rock deformation, International Journal of Rock Mechanics and Mining Sciences, 66, 114-123, 2014.

Crespo, E., Luque, F. J., Barrenechea, J. F., and Rodas, M.: Influence of grinding on graphite crystallinity from experimental and natural data: implications for graphite thermometry and sample preparation, Mineralogical Magazine, 70(6), 697-707, 2006.

Kirilova, M., Toy, V., Timms, N., Halfpenny, A., Menzies, C., Craw, D., Beyssac, O., Sutherland, R., Townend, J., Boulton, C., Carpenter, B., Cooper, A., Grieve, J., Little, T., Morales, L., Morgan, C., Mori, H., Sauer, K., Schleicher, A., Williams, J., Craw, L.: Textural changes of graphitic carbon by tectonic and hydrothermal processes in an active plate boundary fault zone, Alpine Fault, New Zealand. In Gessner, K., Blenkinsop, T.G., Sorjonen-Ward, P., (eds), Geological Society, London, Special Publication 453 'Advances in the Characterization of Ore-Forming Systems from Geological, Geochemical and Geophysical data', in press.

Kuo, L. W., Li, H., Smith, S. A., Di Toro, G., Suppe, J., Song, S. R., and Si, J.: Gouge graphitization and dynamic fault weakening during the 2008 Mw 7.9 Wenchuan earthquake, Geology, 42(1), 47-50, 2014.

Large, D. J., Christy, A. G., and Fallick, A. E.: Poorly crystalline carbonaceous matter in high grade metasediments: implications for graphitisation and metamorphic fluid compositions, Contributions to Mineralogy and Petrology, 116(1-2), 108-116, 1994.

Manatschal, G.: Fluid-and reaction-assisted low-angle normal faulting: evidence from rift-related brittle fault rocks in the Alps (Err Nappe, eastern Switzerland), Journal of Structural Geology, 21(7), 777-793, 1999.

Moore, D. E., and Lockner, D. A.: Crystallographic controls on the frictional behavior of dry and water-saturated sheet structure minerals, Journal of Geophysical Research: Solid Earth, 109(B3), 2004.

Morrow, C. A., Moore, D. E., and Lockner, D. A.: The effect of mineral bond strength and adsorbed water on fault gouge frictional strength, Geophysical Research Letters, 27(6), 815-818, 2000.

Nakamura, Y., Oohashi, K., Toyoshima, T., Satish-Kumar, M., and Akai, J.: Strain-induced amorphization of graphite in fault zones of the Hidaka metamorphic belt, Hokkaido, Japan, Journal of Structural Geology, 72: 142 – 161, 2015.

Di Toro, G., Han, R., Hirose, T., De Paola, N., Nielsen, S., Mizoguchi, K., Ferri, F., Cocco, M. and Shimamoto, T.: Fault lubrication during earthquakes, Nature, 471(7339), p.494., 2011.

~~.Nakatani, M.: Conceptual and physical clarification of rate and state friction: Frictional sliding as a thermally activated rheology, Journal of Geophysical Research: Solid Earth, 106(B7), 13347-13380, 2001.~~

Oohashi, K., Hiros, T. and Shimamoto, T.: Shear-induced graphitization of carbonaceous materials during seismic fault motion: experiments and possible implications for fault mechanics, Journal of Structural Geology, 33.6: 1122-1134, 2011.

Oohashi, K., Hirose, T. and Shimamoto, T.: The occurrence of graphite-bearing fault rocks in the Atotsugawa fault system, Japan: origins and implications for fault creep, Journal of Structural Geology 38: 39-50, 2012.

Oohashi, K., Hirose, T. and Shimamoto, T.: Graphite as a lubricating agent in fault zones: An insight from low-to high-velocity friction experiments on a mixed graphite-quartz gouge, Journal of Geophysical Research: Solid Earth, 118(5), pp.2067-2084, 2013.

Pimenta, M.A., Dresselhaus, G., Dresselhaus, M.S., Cancado, L.G., Jorio, A. and Saito, R.: Studying disorder in graphite-based systems by Raman spectroscopy, Physical Chemistry Chemical Physics, 9(11), pp.1276-1290, 2007.

Rietmeijer, F. J., and Mackinnon, I. D.: Poorly graphitized carbon as a new cosmothermometer for primitive extraterrestrial materials. Nature, 315(6022), 733-736, 1985.

Rutter, E.H., Hackston, A.J., Yeatman, E., Brodie, K.H., Mecklenburgh, J. and May, S.E.: Reduction of friction on geological faults by weak-phase smearing, Journal of Structural Geology, 51, pp.52-60, 2013.

Savage, R. H.: Graphite lubrication, Journal of Applied Physics 19.1: 1-10, 1948.

Toy, V.G., Niemeijer, A.R., Renard, F. Wirth, R., and Morales, L.: Striation and slickenline development on quartz fault surfaces at crustal conditions: origin and effect on friction, Journal of Geophysical Research, doi: 10.1002/2016JB013498, in press.

Tuinstra, F. and Koenig, J.L.: Raman spectrum of graphite, The Journal of Chemical Physics, 53(3), pp.1126-1130, 1970.

White, S. H., Burrows, S. E., Carreras, J., Shaw, N. D., and Humphreys, F. J.: On mylonites in ductile shear zones, Journal of Structural Geology, 2(1-2), 175-187, 1980.

Wopenka, B., and Pasteris, J. D.: Structural characterization of kerogens to granulite-facies graphite: applicability of Raman microprobe spectroscopy, The American Mineralogist, 78(5-6), 533-557, 1993.

Zulauf, G., Kleinschmidt, G., and Oncken, O.: Brittle deformation and graphitic cataclasites in the pilot research well KTB-VB (Oberpfalz, FRG), Geological Society, London, Special Publications, 54(1), 97-103, 1990.

Table 1. Summary of the conditions at which experiments were carried out and results.

Table 2. Summary of the relationship between shear strain and average R2 within a sample. The conditions of each experiment are also given as follows: applied normal stress in MPa, ~~slip rates~~sliding velocities in μm/s and sliding displacement in mm.

Figure 1. Plots of mechanical data (a) friction coefficient, μ vs. displacement (b), (c), (d) friction coefficient, μ vs. shear strain.

Figure 2. Representative Raman spectra illustrating: (i) the most crystalline graphite (left column) within a sample; (ii) graphite with ~~approximate~~ average crystallinity per sample (middle column); and (iii) the most disordered graphite (right column) encountered in each sample. The R2 ratio for each spectrum is also noted in italic font.

Figure 3. Plot of the average R2 ratio vs shear strain accumulated during each experiment.

Figure 4. SEM images, obtained from the deformed graphite gouge during experiment 8 (normal stress at 25 MPa with 1 μm/s sliding velocity), show: (a) Slickenlines ornamenting the shear surface; (b), (c) A well-compacted layer of aligned graphite grains, which make up the shear surface. Bright patches due to a differential charging effect; (d) A less deformed zone with typical cataclastic fabric, underlying the shear surface; (e) Dilated cleavage planes in large graphite grains filled with smaller platy graphite grains oriented sub-perpendicular to the shear direction; (f) Fractured graphite grains.

Supplementary material 1 (S1). Raman data from 20 spectra per sample together with calculated R2 ratio and average R2 value for each sample. The last column represents temperature estimated by the current best calibration of a Raman-based thermometer: $T\ (^{o}C) = -445 * R2 + 641 \pm 50$.

Experiment number	Normal stress (MPa)	Sliding velocity (µm/s)	Displacement (mm)	Peak friction coefficient (μ_{peak})	Steady state friction coefficient (μ_{ss})	Shear strain maximum
1	5	1	20	0.53	*0.22*	17.70
2	5	1	10	0.53	0.22	8.17
3	5	1	5	0.52	*not reached*	4.23
4	5	10	20	0.53	0.24	20.45
5	5	100	20	0.57	0.22	16.89
6	5	100	10	0.55	0.22	9.80
7	5	100	5	0.57	*not reached*	3.87
8	25	1	20	0.43	0.17	21.45
9	25	10	20	0.43	0.17	31.86
10	25	100	20	0.41	0.14	46.77

Table 1. Summary of the conditions at which experiments were carried out and results.

Sample	Experimental conditions	Shear strain	Average R2 (error estimate ± 0.05)	Total frictional work
Pre-shear graphite	N/A	N/A	0.173	
Exp. 2	5 MPa, 1 μm/s, 10 mm	8.17	0.438	38.8689
Exp. 6	5 MPa, 100 μm/s, 10 mm	9.80	0.430	46.6369
Exp. 5	5 MPa, 100 μm/s, 20 mm	16.89	0.454	157.9314
Exp. 1	5 MPa, 1μm/s, 20 mm	17.70	0.506	165.4748
Exp. 4	5 MPa, 10 μm/s, 20 mm	20.45	0.517	180.8346
Exp. 8	25 MPa, 1 μm/s, 20 mm	21.45	0.520	192.9007
Exp. 9	25 MPa, 10 μm/s, 20 mm	31.86	0.580	283.7721
Exp. 10	25 MPa, 100 μm/s, 20 mm	46.77	0.604	424.0356

Table 2. Summary of the relationship between shear strain ~~and~~, average R2, and total frictional work within a sample. The conditions of each experiment are also given as follows: applied normal stress in MPa, ~~slip rates~~sliding velocities in μm/s and sliding displacement in mm.

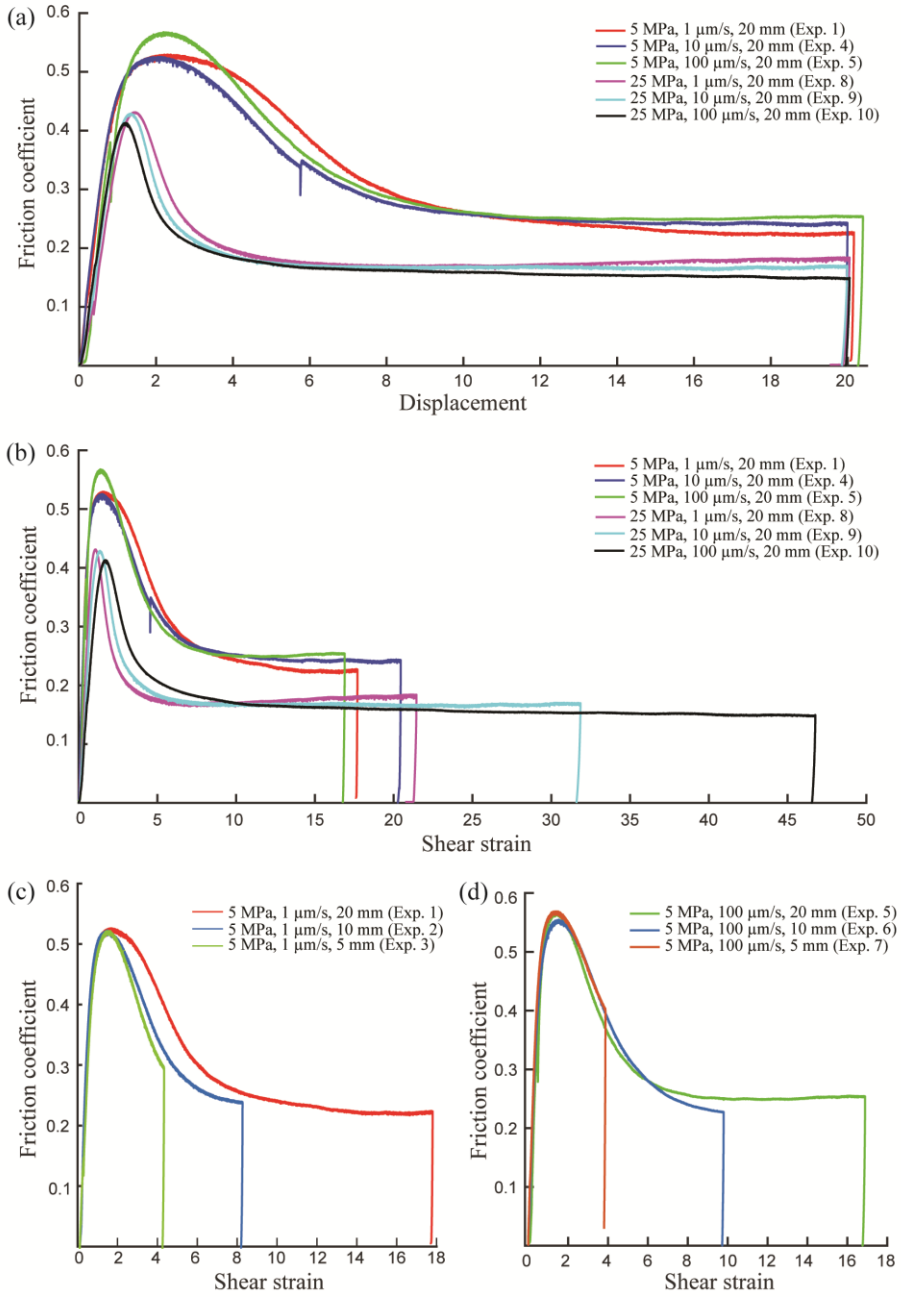

441

442 **Figure 1**. Plots of mechanical data (a) friction coefficient, µ vs. displacement (b), (c), (d) friction coefficient, µ vs. shear
443 strain.

444

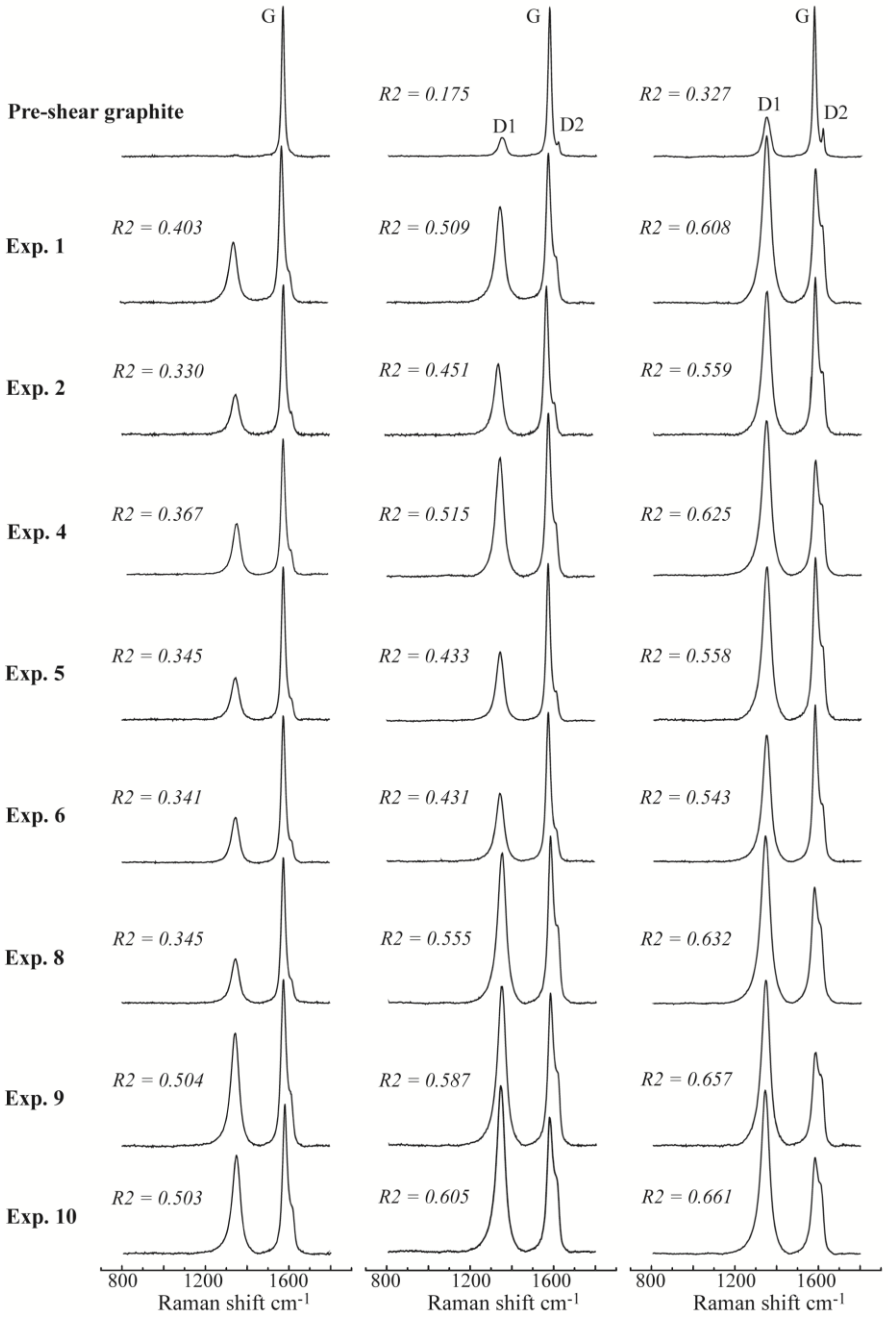

Figure 2. Representative Raman spectra illustrating: (i) the most crystalline graphite (left column) within a sample; (ii) graphite with ~~approximate~~ average crystallinity per sample (middle column); and (iii) the most disordered graphite (right column) encountered in each sample. The R2 ratio (with an error estimate of 0.05) for each spectrum is also noted in italic font.

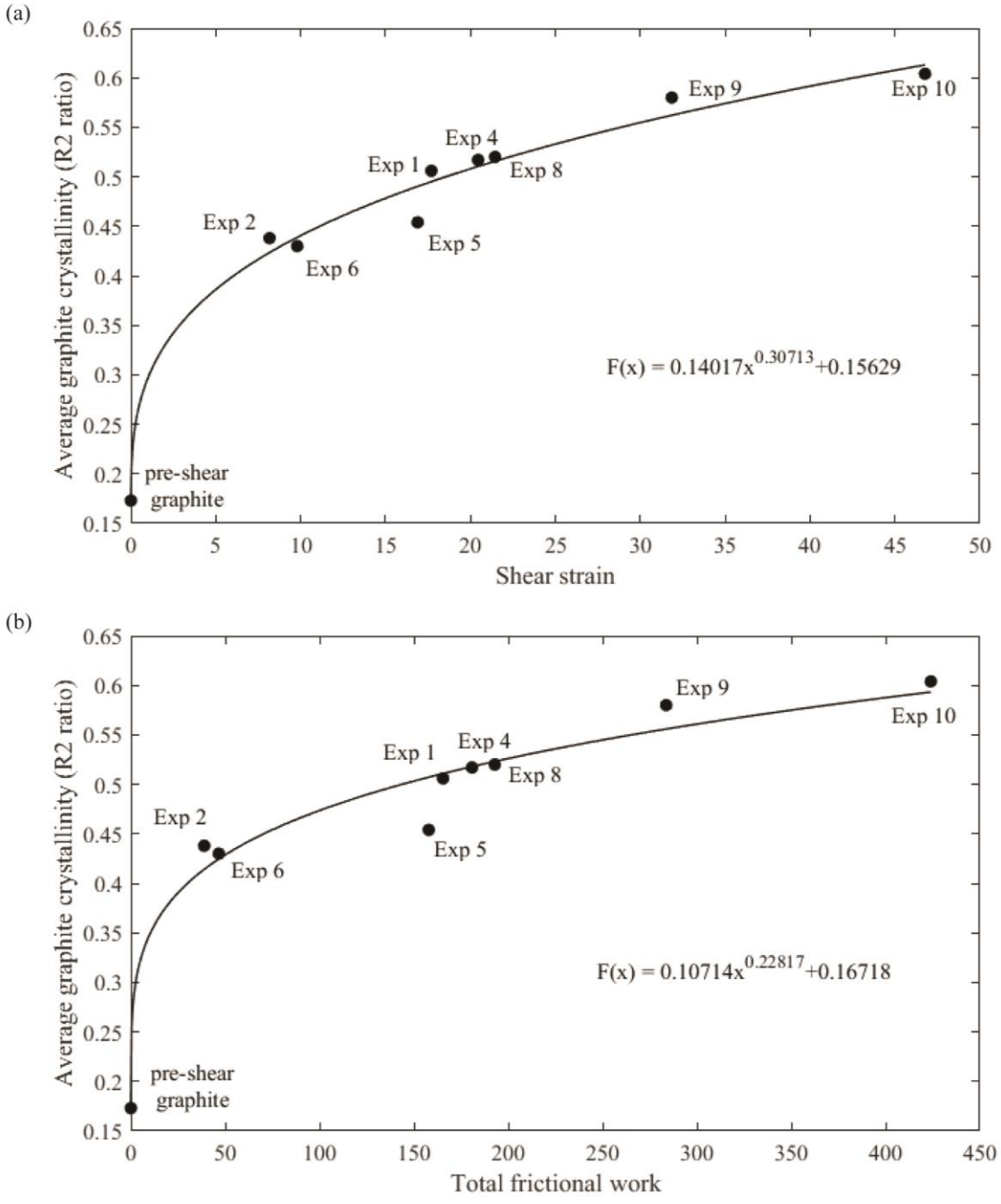

Figure 3. **(a)** Plot of the average R2 ratio vs shear strain accumulated during each experiment. **(b)** Plot of the average R2 ratio vs total frictional work during each experiment.

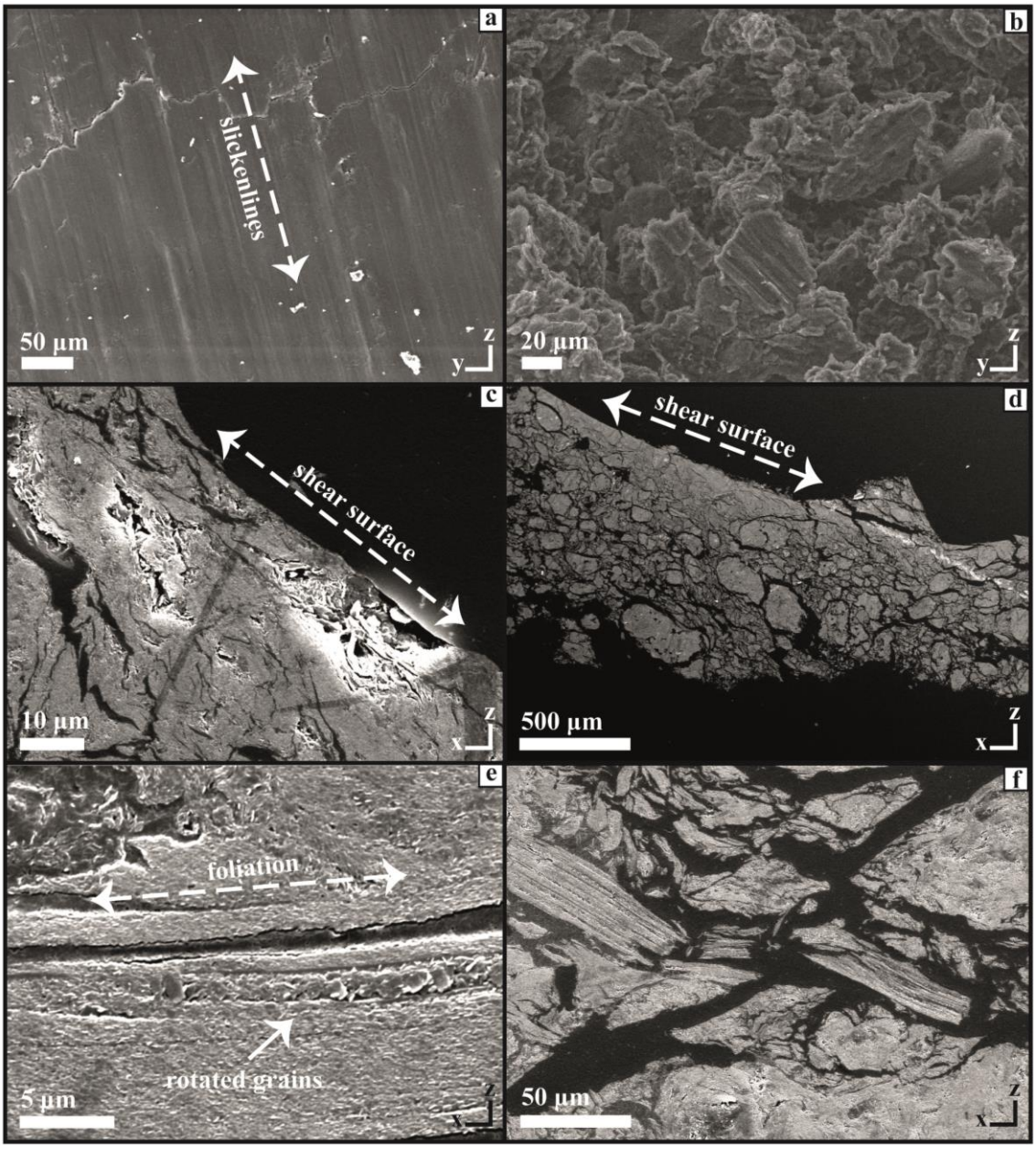

454

455 **Figure 4.** SEM images, obtained from the deformed graphite gouge during experiment 8 (normal stress at 25 MPa with 1
456 µm/s sliding velocity), show: (a) Slickenlines ornamenting the shear surface; (b), (c) A well-compacted layer of aligned
457 graphite grains, which make up the shear surface. Bright patches due to a differential charging effect; (d) A less deformed
458 zone with typical cataclastic fabric, underlying the shear surface; (e) Dilated cleavage planes in large graphite grains filled
459 with smaller platy graphite grains oriented sub-perpendicular to the shear direction; (f) Fractured graphite grains.

460

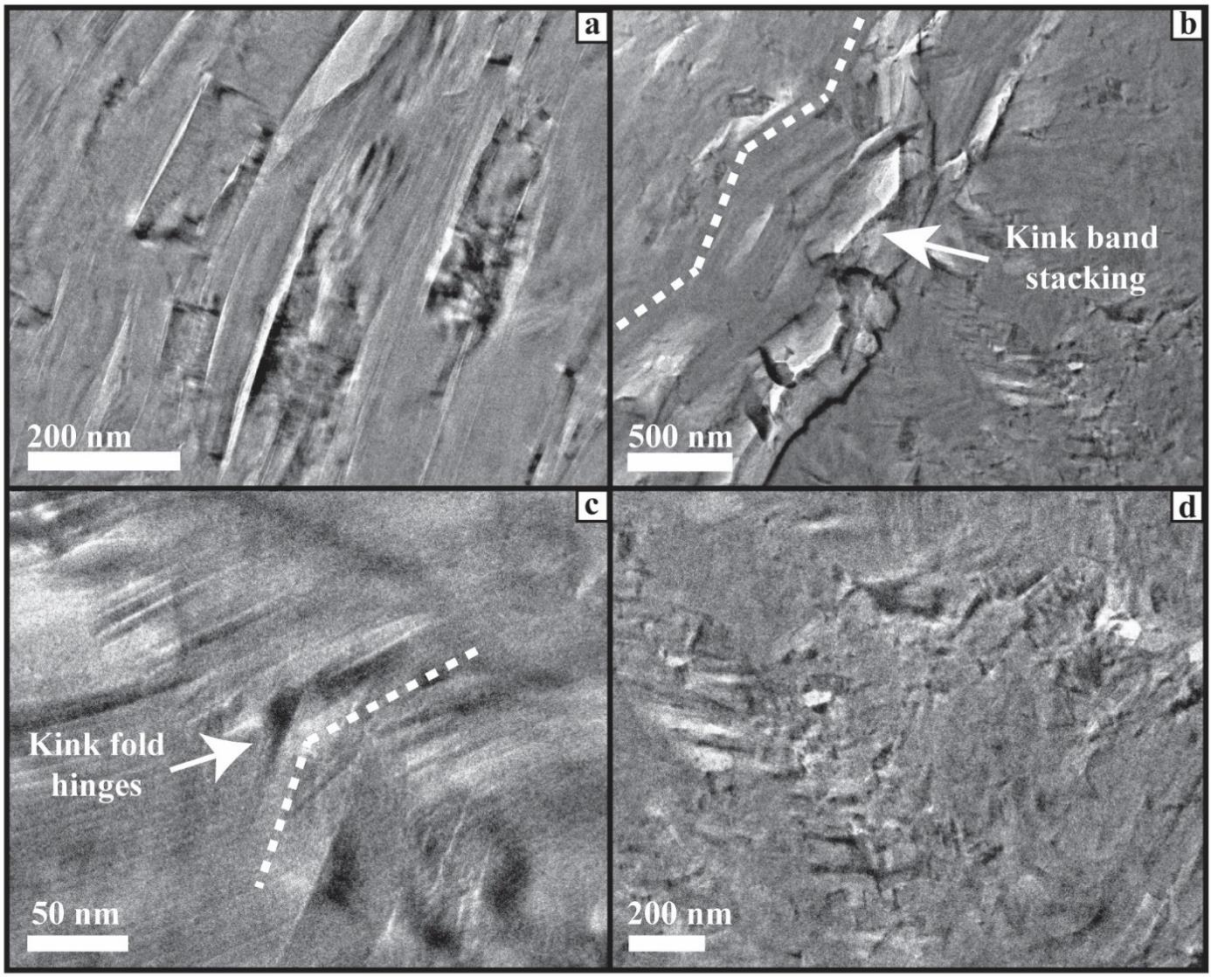

Figure 5 TEM images showing microstructural characteristics of the slip-localized shear surface: (a) aligned grains showing slightly different orientation; (b) kink band stacking; (c) dilated kink fold hinges; (d) fragmented grains.